ISSN: 0067-2904

Evaluation and Delineation of Sulfur Groundwater Leakages Using Electrical Resistivity Techniques in Hit Area, Western Iraq

Osama J. Mohammed, Ali M. Abed*, Mohammed A. Alnuaimi
Department of Applied Geology, College of Science, Anbar University, Ramadi, Iraq

Received: 2/8/2020 Accepted: 29/9/2020

Abstract

Electrical resistivity methods are one of the powerful methods for the detection and evaluation of shallower geophysical properties. This method was carried out at Hit area, western Iraq, in two stages; the first stage involved the use of 1Dimensional Vertical Electrical Sounding (VES) technique in three stations using Schlumberger array with maximum current electrodes of 50m. The second stage included the employment of two dimension (2D) resistivity imaging technique using dipole-dipole array with a-spacing of 4m and n-factor of 6 in two stations. The 1D survey showed good results in delineating contaminated and clear zones that have high resistivity contrast. Near the main contaminated spring, the 2D resistivity imaging technique was applied in four sections length (100 m) using a dipole-dipole array position coincided with the three points VES. We compared the results of the interpretation of imaging the techniques 2D and VES. We found that the 2D imaging resistivity technique was better than VES survey in determining the distribution of pollution under the surface in the area surveyed. It was also found that the polluted water is located about 5 m below the surface. The largest amount of leakage was found towards the northeast and coincided with the direction of the groundwater movement. Spring water has leaked from outside the region through the Kubaisah area. Most of this water is contained in quaternary deposits and karst gypsum fractures.

Keywords: Resistivity method**,** Contaminated spring, Fatha Formation**,** Hit-western Iraq**.**

تقييم وتحديد تسربات المياه الجوفية الكبريتية باستخدام تقنيات المقاومة النوعية الكهربائية في منطقة هيت ، غرب العراق

اسامه جاسم محمد، علي مشعل عبيد*، محمد احمد علي
قسم الجيولوجيا التطبيقية, كلية العلوم, جامعة الانبار

الخلاصه

طرق المقاومة الكهربائية هي واحدة من الطرق المميزة لاكتشاف وتقييم التحريات الجيوفيزيائية الضحلة. تم تنفيذ تقنيات المقاومة الكهربائية في منطقة هيت غربي العراق على مرحلتين. المرحلة الأولى باستخدام تقنية الجس الكهربائي العمودي في ثلاث محطات باستخدام ترتيب شلمبرجير بنشر اقطاب لمسافة تبلغ 50 م. المرحلة الثانية هي تقنية التصوير ثنائي الأبعاد للمقاومة النوعية باستخدام ترتيب ثنائي القطب – ثنائي القطب مع تباعد بين القطاب 4 م. نتائج لمسح الجس الكهربائي العمودي جيدة في تحديد المناطق الملوثة حيث تكون

*Sc.amah_mishal@uoanbar.edu.iq

واضحة عندما يكون هناك تباين عالي في المقاومة بينها وما يحيط بها. بالقرب من الينبوع الرئيسي الملوث ، تم تطبيق تقنية تصوير المقاومة ثنائية الأبعاد في أربعة مسارات بطول (100 م) لكل منها، باستخدام ترتيبة ثنائية القطب– ثنائي القطب عند النقاط الثلاث للجس الكهربائي العمودي. مقارنة نتائج تفسير تقنيات التصوير ثنائي البعد و الجس الكهربائي العمودي تبين أن تقنية التصوير ثنائي الابعاد للمقاومة هي الأفضل في تحديد توزيع التلوث تحت السطح في المنطقة التي تم مسحها. حيث أن المياه الملوثة تقع على عمق 5 م. أن أكبر كمية تسرب وجدت في اتجاه الشمال الشرقي تزامنا مع اتجاه حركة المياه الجوفية ومن خارج المنطقة عبر منطقة الكبيسة. يتم احتواء معظم هذه المياه في الرواسب الرباعية وكسور الجبس الكارستية لتكوين الفتحة (المايوسين الاوسط).

Introduction

Electrical resistivity method was applied to characterize the area contaminated with hydrocarbons, due to its importance economically and environmentally. Economically, this method is used for avoiding the contaminated water area and using the clean water area to dig wells, as well as setting appropriate requirements to prevent the spread of contamination. Environmentally, it is used to determine the area of sulfur dioxide pollution, its geographical extent, and its health impact on humans, animals and plants. Hussien *et al*. [1] pointed out that there is an important relationship between the continuous emission of sulfur dioxide and its sources from sulfur fountains and sewage in the city of Hit. The spatial distribution maps of hydrogen sulfide (H_2S) showed that 38% of Hit's area is exposed to the concentration of this compound with the influence of bad smell. Hydrocarbon pollutants are likely to exhibit low-resistivity anomalies. The entry of hydrocarbons through the soil leads to a salty halo around these compounds [2- 11]. Anomalies of intense resistivity due to the presence of an insulating hydrocarbon layer on the water surface results in the effect of noise on electrical measurements ([12, 13].

Imaging techniques have been proven to be powerful in groundwater pollution studies [14]. New inversion algorithms were used to produce electrical images, which can represent a realistic 2D or 3D system. Electrical imaging includes the measurement of a series of constant separation traverses (CST) or vertical electrical sounding (VES) with increased electrode spacing depending on the type of electrode arrays to achieve data from large depths. Several authors have used the electrical resistivity techniques to evaluate and delineate the groundwater leakages. Shevnin *et al*. [6] used the sounding resistivity technique that acts as an electrical resistivity tomography (ERT) technique. This has been applied to demonstrate that oil pollution in the ground alters the resistivity of groundwater and the surrounding rocks. In addition, it appears as a low-resistivity region so that the resistivity sounding can be estimated horizontally and vertically, along with its location, lithology, pollution sources, potential migration paths, and the degree of pollution. Shevnin *et al*. [7] used VES method on 2D resistivity imaging technology and 2D interpretation at an oiled site in Tabasco, Mexico. The polluted areas were characterized by low-resistivity abnormalities, which allowed the estimation of the value of the boundary resistivity separating the clean and polluted areas. This made the method useful for a more accurate and detailed determination of the polluted areas. Allen *et al*. [10] provided a detailed spatial analysis of the microbial community structure in an ancient underground oil column at the site of a former refinery in Carson City, Michigan. Initial microbiological measurements showed that high levels of hydrocarbon-soluble microbial groups can coincide with peak hydrocarbon contamination and high electrical conductivity levels. Uchegbulam and Ayolabi [11] used the 2D electrical resistivity tomography in investigating groundwater pollution in Sapele area, Nigeria. The results showed that the subsurface is characterized with soil material with resistivity ranging from 42 - 15,000 Ω·m, reflecting varying degrees of conductivity associated with changing lithology and fluid type. This low conductivity formations can be attributed to hydrocarbons, which is an indication that the shallow aquifer in the study area has been polluted.

Thabit and Khalid [15] suggested that the 2D imaging technique is a successful and powerful tool in separating contaminated zones from clear ones and in detecting underground seepage depth and the moving direction in southeast of Karbala city, Iraq. As for engineering studies of karst phenomena in the Hit region, field electric surveys were applied using Bristow method and 2D resistivity imagining technology [16- 19]. These studies showed subsurface caves and fractures in different shapes and sizes

in the layers of gypsum rocks. They represented weak packages that may lead to risks in government and residential buildings. Karst subzone was reported to facilitate the transmission of sulfur water in large areas of the city of Hit.

The objectives of the study include evaluating the usability of the vertical electrical sounding and 2D resistivity imagining techniques to determine the contamination with hydrocarbon materials in groundwater. We also aimed at the evaluation and delineation of the clean and contaminated areas according to the limits of the insulating resistivity values.

Materials and Method

Site description

The study area lies within Hit area, western of Al-Anbar governorate. There is a seepage problem in the site of water contaminated with hydrocarbons. This problem is distributed in different areas of the city of Hit (Figure-1), the largest of which is an area of exudation that represents a spring for contaminated water, which is considered as a touristic area while its waters are used as a treatment for some skin diseases. This area is located in the southern part of Al-Jezira district along the right bank of Euphrates River.

Figure 1-Satellite image showing the location of the study area

Fatha Formation (Middle Miocene) represents the main geological outcrop in the area. Fatha Formation is exposed in the most parts of the Western desert regions. It is divided into four members described as follows [20]; First, a Lower Member that was developed east of Euphrates and in the narrow strip along the south bank of the river, and consists of green marl, limestone and gypsum. Second, an Upper Member that was developed east of Euphrates, especially along Lake Tharthar. The thickness of this member ranges from 20-30 m. It consists of marl, limestone, gypsum, clay stone, and sandstone. Third, the Nfayil Member which is exposed only south of Euphrates River and covers large parts of the region. The beds consist of green marl and limestone. The second course contains oysters, which is a diagnostic feature of the Nfayil family. Its thickness ranges between 5-18 m. Forth, the Clastic Member that was developed in the southeastern part only. It consists of marl, clay stone and fine sandstone with secondary gypsum in a rhythmic nature. The thickness of this member ranges from 10-15 m. A thin layer of limestone may occur at the bottom. Al-Ghurery [21] divided the stratigraphic sequence of Fatha Formation in the Hit region into interbedded clay and siltstone, marl, and thick gypsum rocks (Figure-2).

AGE	FORMATION	THICKNESS (m)	LITHOLOGY	DESCRIPTION
Middle Miocene	Fatha	4		Massive gypsum, white in colour
		2		Greenish to yellowish marl with intercalation of anhydrite weathered in places.
		6		Silty claystone with intercalation of siltstone, yellowish to redish in colour, with thin bed of gypsum.

Figure 2-Lithological setting of Fatha Formation in Hit area [21]

Hydrogeological conditions

The hydrogeological conditions in the study area are part of the regional hydrogeological settings, which are controlled structurally by the regional basin depositions of the Upper Oligocene–Quaternary sediments [22].

The hydrogeological situation was described in a separate hydrogeological system [23,24] classified into three hydrogeological units, where these units are characterized by conditions not limited to the feeding area as well as a semi-confined state in a limited state in the discharge area (Figure-3a). The first unit consists of the prospects for carrying water from the Quaternary sediments, involving mainly silt, sand, gravel, gravel, and sandstone. It is described by local non-limited extension of the state of the banking storage located along the banks of Euphrates River, with a range of permeability coefficient between 5 and 15 m / day. The second unit consists of the prospects for carrying water which is made up of porous limestone and gypsum fractures characterized by the status of semi-confined in a narrow case of a small stretch. The permeability coefficient for these horizons ranged between 1 and 5 m / day. The third unit of water-bearing horizons consists of Euphrates, Ana and Baba formations, which consist of limestone, crushed porous and broken dolomite. The permeability of the unit ranged between 4 and 50 m / day. The flow behavior and motion of groundwater in the study area (Figure-3b) illustrates a common pattern of groundwater in the direction of ENE, slightly deviated to the directions of NE and SE, which is caused by local geomorphological and structural phenomena, reflected as a division of groundwater.

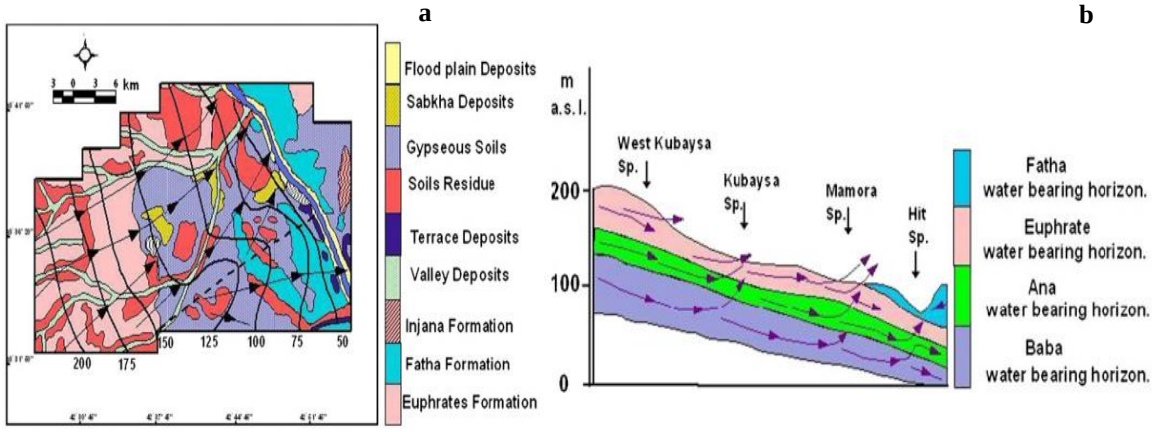

Figure 3-Hydrogeologic map and section within Hit–Kubaiysa region [23]

Data acquisition

The study included a description of the situation of the natural source bed in the studied area. The pollutants can migrate to reach the surface through weak areas. The surface source of pollution in the studied area (at the present time) is the most important and dangerous because of a large amount of pollutants constantly flow from the contaminated springs that penetrate the top soil to reach the groundwater and then pollute the shallow groundwater layers.

The field work was carried out using Terrameter SAS 4000 resistivity meter and included two stages.

A- The first stage: The application of the VES technique using Schlumberger array in three stations (VESA1, VESA3 and VESB1). The aim of this work is to understand the distribution and the direction of leakage movement.

B- The second stage: The application of the 2D resistivity imaging method using dipole-dipole array with a-spacing of 4 m, in 4 stations (A1, A2, B1 and B2). At each station, 25 electrodes were used along 100 m with electrode spacing of 4 m and n-factor of 6.

The VES survey focused on the same area covered in the first work step. VES, at three VES points, was used to cover the area around the main contaminated spring. The software IPI2Win was used in the interpretation of VES points.

2D Inverse modeling was carried out using the RES2DINV ver. 4.9.15 Software, with the standard least-squares method. The reading points of dipole-dipole array with a spacing of 4 meters are 226 readings**.**

Results and discussion

VES points

In a qualitative interpretation, there are three techniques used to interpret the three sounding curves distributed along a profile (A-A '). The first technique is to study the types of VES curves. The vertical differences curve can reflect the distribution of resistivity values below the surface in the study region. Therefore, this interpretation technique provides preliminary information about the number of electrical horizons for each curve, where the preparatory point in the field curve, which reflects changes in electricity, can notice the increase and decrease in the resistivity values [25]. The values for each horizon are compared to each other. The field curves in the studied area were categorized into the following groups:

a – Group (QQHA): This QQHA-type appeared in two VES points, which are VESA1 and VESA3, as shown in Figures-4 and 5, respectively. These points represent six electrical horizons. The first and second horizons are represented by gypsum rocks with 17.8 and 17.9 Ω.m, respectively. While the second horizon represents low resistivity values of the partially saturated zone that is located above water table. The third horizon is characterized by lower resistivity values because it is located under water table; therefore it reflects the presence of Fatha Formation, which consists of marl, limestone, gypsum, clay stone, sandstone and sandstone. The fourth, fifth and sixth horizons show gradually increased apparent resistivity values that are correlated with the depth.

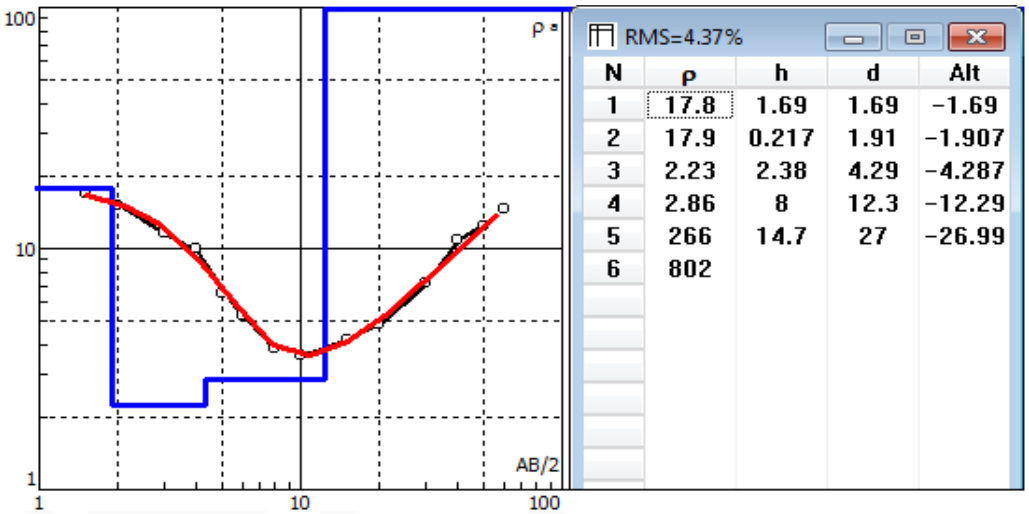

N	ρ	h	d	Alt
1	17.8	1.69	1.69	-1.69
2	17.9	0.217	1.91	-1.907
3	2.23	2.38	4.29	-4.287
4	2.86	8	12.3	-12.29
5	266	14.7	27	-26.99
6	802			

Figure 4 -The results of inverse modeling method for VESA1 point.

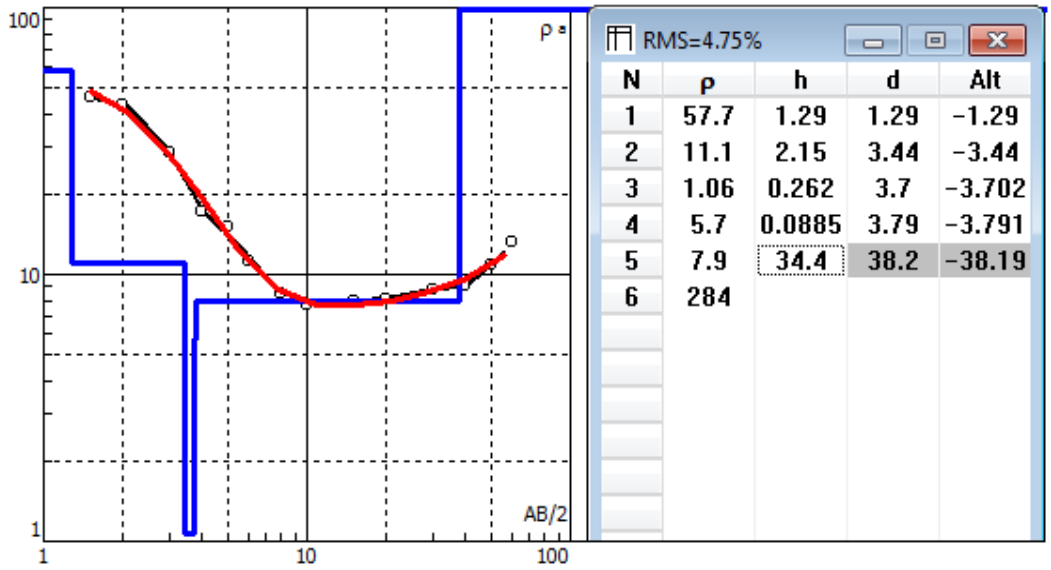

N	ρ	h	d	Alt
1	57.7	1.29	1.29	-1.29
2	11.1	2.15	3.44	-3.44
3	1.06	0.262	3.7	-3.702
4	5.7	0.0885	3.79	-3.791
5	7.9	34.4	38.2	-38.19
6	284			

Figure 5 The results of inverse modeling method for VESA3 point.

b – Group (QQQHAA): The QQQHAA-Type appeared in VESB1, as shown in Figure-6. It is represented by seven electrical horizons. The thin surface of the dry soil layer (0.827 thickness) has relatively high resistivity values compared with the second, which has 20.7 **Ω**.m of gypsum rocks with 1.66 m thickness. The third horizon represents the third part of the gypsum rock affected by moisture. The fourth horizon, which represents low resistivity values, may be caused by the presence of the partial saturation zone of marly interbedded with thin beds of gypsum. The fifth electrical horizon is of a relatively high resistivity value compared with that of the second horizon. The fifth horizon has a lower resistivity value while the sixth and seventh ones have high values. The stratigraphic sequence adjacent to the Point VESB1 is located below the area saturated with sulfur water. The stratification sequence is composed of clay stone, sandstone and sandstone.

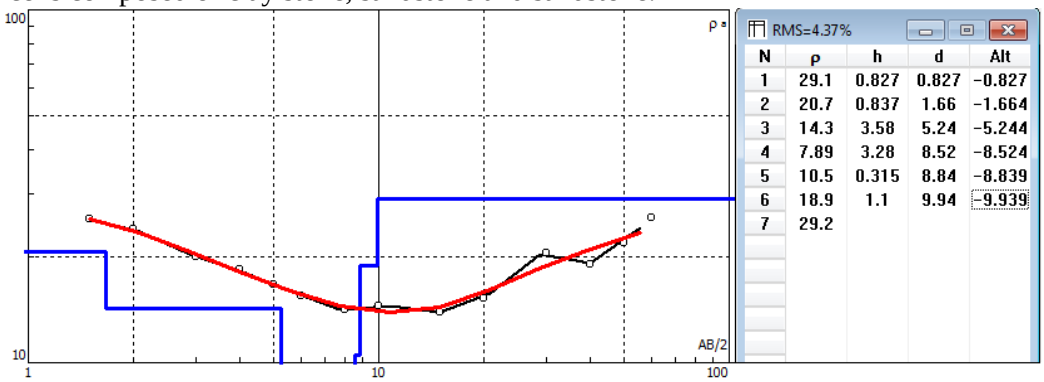

N	ρ	h	d	Alt
1	29.1	0.827	0.827	-0.827
2	20.7	0.837	1.66	-1.664
3	14.3	3.58	5.24	-5.244
4	7.89	3.28	8.52	-8.524
5	10.5	0.315	8.84	-8.839
6	18.9	1.1	9.94	-9.939
7	29.2			

Figure 6-The results of inverse modeling method for VESB1 point.

A section of apparent resistivity or a pseudo cross-section gives introductory information about changes in the values of apparent resistance with the increase in the disconnection of the half-current (AB / 2). However, three apparent resistivity sections were drawn in this technique using IPI2win along the A –A ' profile. The apparent resistivity section (A –A ') passes along the three VES points, as shown in Figure-6a.

The geo-electrical section (A –A ') passes through the vertical electrical sounding points (VESA1, VESA3, VESB1), as shown in Figure-6b. It is supported by a stratum column of the detector located at the VESB1 point (Figure-7). This is represented by the bottom sequence from the bottom to up, where the lower part is represented by clay stone (reddish brown, hardtop firm) to brownish yellow and hard limestone bed. It is followed by yellowish marl interceded with beds of gypsum. The last and highest part is made of a massive bed of gypsum interceded with oil seeps.

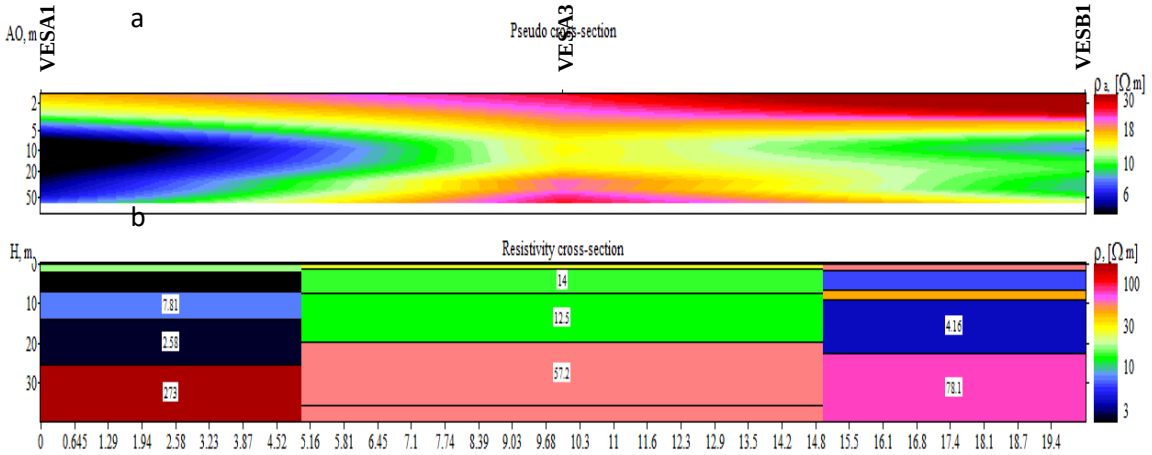

Figure 6-Pseudo cross-section (a) and resistivity cross-section (b) passing along A-A' profile.

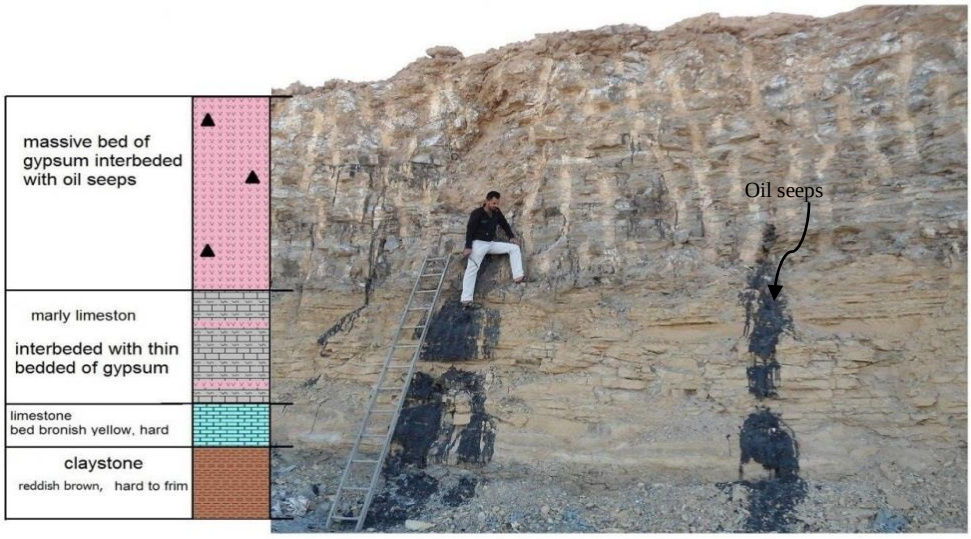

Figure 7-The stratigraphic column of an outcrop in the area [26].

The First Geo-Electrical Horizon is represented by a thin soil layer and characterized by lateral variations of resistivity ranging between 17.7Ω.m in the VESA1 point to 57.7 Ω.m at VESB1. This variation in the resistivity values may be caused by the lithological changes in composition and farness or nearness of the oil-contaminated water from the surface of the Earth. The second horizon represents the white plaster layer that is dissolved in some areas due to the leakage of groundwater or rainwater from the surface of the earth. This is evident at the point VESA1 which shows the accumulation of water contaminated with hydrocarbons characterized by low values of resistivity (4.05 Ω.m) at this horizon, while the value is 2.27 Ω.m at the third horizon. As for the same two horizons at the VESA3 point, the resistivity values increase to 14.7 Ω.m and 14.6 Ω.m for the first and second horizons, respectively. This is due to the influence of moisture. The second horizon at point VESB1 is marked with a value as low as 11.1 μm, as it is affected by moisture. It is clear that the leakage of groundwater contaminated with oil materials is concentrated at the VESA1 point region. The flow of contaminated water from a spring which is about 40 m away from this point confirms these results (Figure-8).

The deeper horizons are represented by silty claystone rocks, according to the stratified column near the point VESA1, which is characterized by very high resistivity values that indicate its high

drought. It is believed that the source of this polluted water is located far from the study area. Whereas, VESA3 and VESB1 are characterized by lower values due to the change of the rocky area in this direction as well as the influence of water and moisture leakage from the accumulation of polluted water at VESA1.

2D Inverse of Dipole-dipole Data

Field data were processed with the RES2DINV 4.9.15 software package to create a 2D electrode [27]. RES2DINV is a computer program that automatically creates 2D designs. The distribution profile of the subsurface resistivity values was characterized using data obtained from a two-dimensional electrical survey [28], after cleaning and removing bad data in two stages; the first stage was building a profile for data points and choosing bad data in a manual mode (Figure-9a). The second stage is using the RMS error option to cut-off the bad data and the improvement of the total of the RMS errors using an automatic statically method through removing the data-points with a large percentage difference (Figure-9b). One of the advantages of this program is that the damping factor, if the data set is very noisy, a relatively larger damping factor is used. If the data set is less noisy, a smaller initial damping factor is used. Flatness filters can be custom-made to fit the types of field data [27].

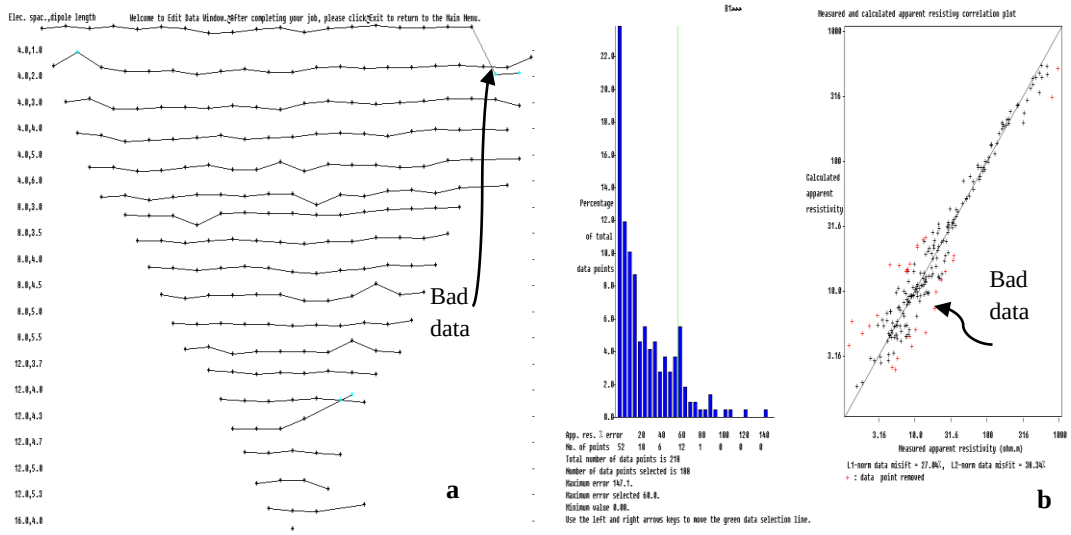

Figure 9-Bad data points of Dipole-dipole array traverse A2; a- Picking the bad data manually. B-Automatic statical way of removing data-points with large percentage differences.

The inverse results of the 2D imaging and the 2D resistivity imaging of then dipole-dipole data along traverses A1, A2, B1, and B2 are shown in Figures- 10 and 11, respectively. The results clearly indicate the contrast variance between the anomalous part of the weak zone and the background resistivity values. Inverse 2D models indicate that sulfur water is located near the surface of the earth as well as within the Quaternary Era deposits and the fractures and caverns of gypsum rocks of Fatha Formation (Miocene). When a hydrocarbon mixes with water, it shows a low resistance zone, but when it dries up it shows a high resistance area. The inverse models (Figures- 10 and 11) show the direction of the profile (EW, NW-SE) for each side.

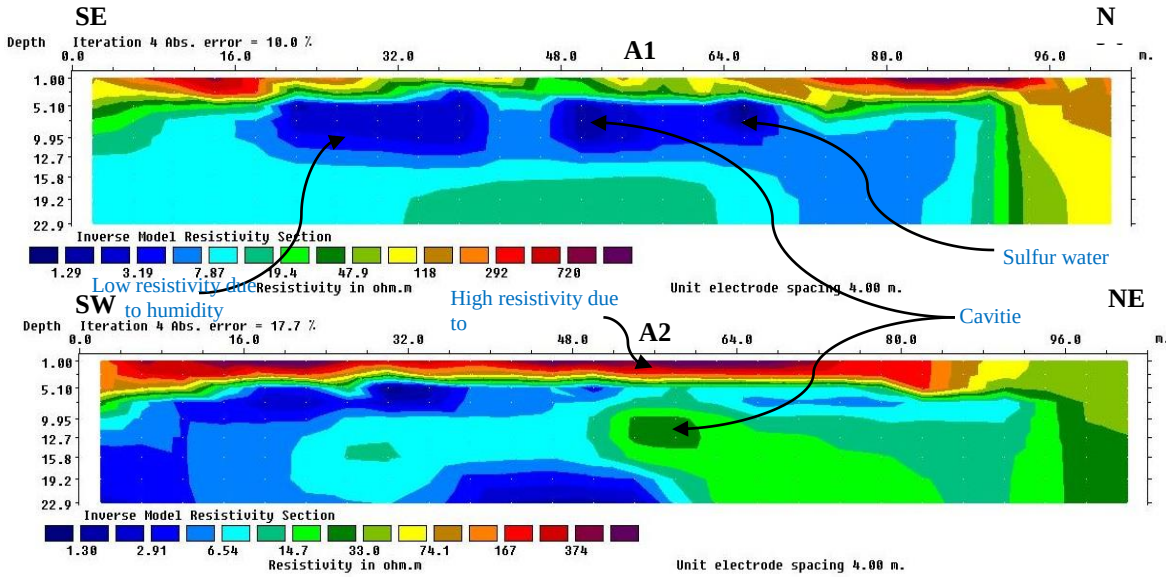

Figure 10 -The inverse model of Dipole-dipole resistivity section at A1 and A2 stations with Standard Least-Squares Inversion Method

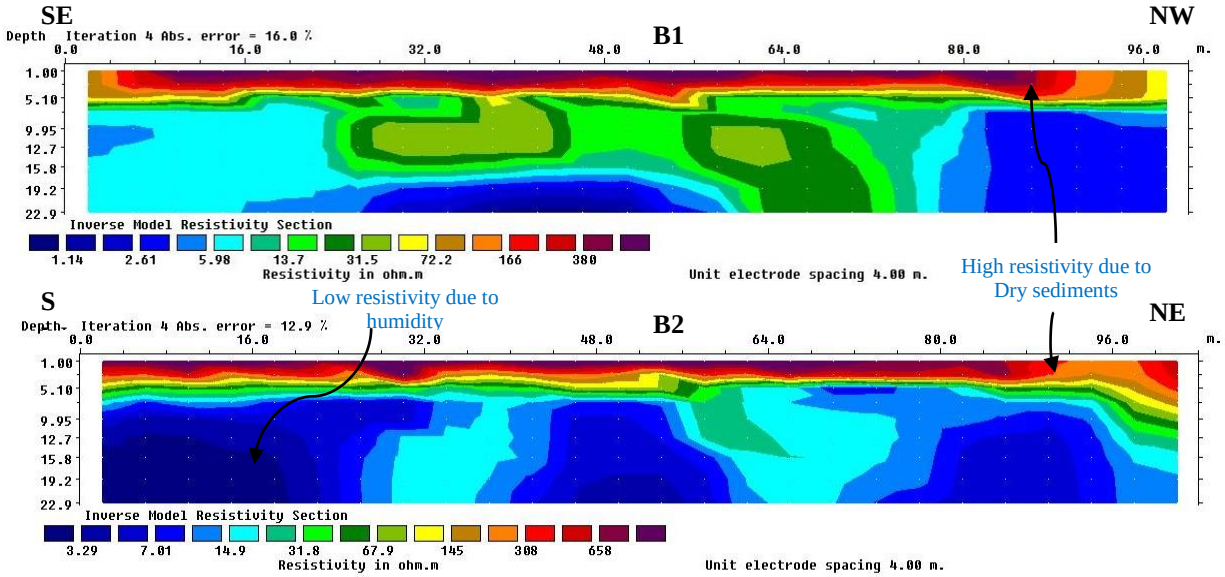

Figure 11-The inverse model of Dipole-dipole resistivity section at B1 and B2 stations with Standard Least-Squares Inversion Method

As Figure-10, the cross-section (A-A ') produced by the vertical electrical sounding interpretation of points VESA1, VESA3 and VESB1 is shown. The two resistivity techniques for determining the presence of sulfur water showed almost identical results. These results indicate that the source of this polluted water is located outside the study area. These conclusions support the results of a previous work [22], as they confirmed that the sulfur water, in the form of springs in the Hit area, was caused by the leakage from outside the region through Kubaiysa area (Figure-2). They also confirmed that most of this water is present in the Quaternary Era sediments, which exist in parts of the study area along with fractures of karst gypsum. The 2D inverse models also show the presence of a clearing area including fractures and caves with gypsum rocks. These caves and fractures are formed as a result of dissolving gypsum rocks with water infiltrated through them, in addition to the rainwater leaking from the surface. Also, it was found that the polluted water is located about five meters below the surface. The largest amount of leakage was found towards the northeast, which coincided with the direction of groundwater movement.

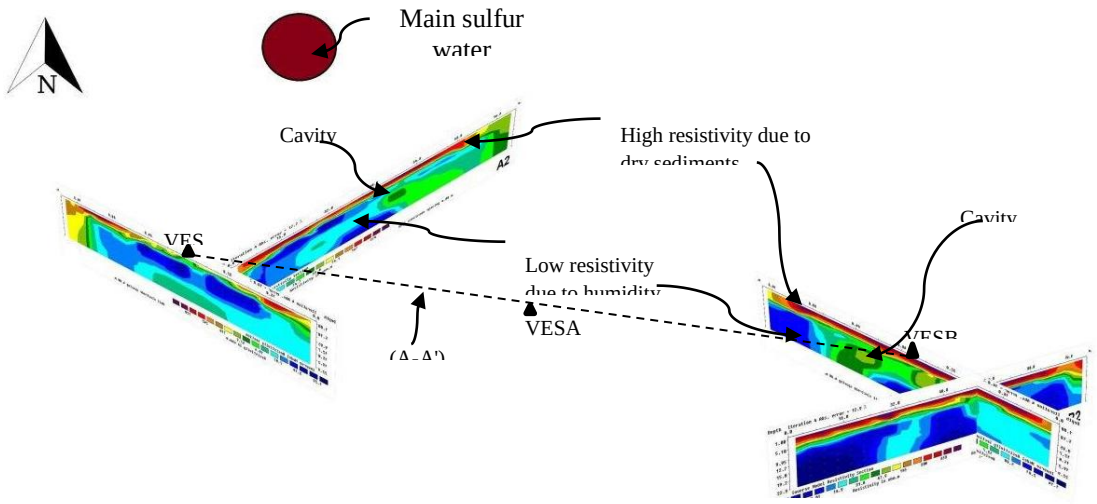

Figure- 10 3D view of 2D Inverse models of Dipole-dipole

Conclusions

Two electrical resistivity techniques were applied to understand, evaluate and delineate the groundwater seepage within Hit area. The results of the VES technique showed the distribution of the subsurface resistivity values between the contaminated area and the surrounding area. The investigation found that the results of the VES survey (Schlumberger array) provided a clear identification of the contaminated areas. On the other hand, the 2D inverse models (Dipole-dipole) indicated that the contaminated zone within the hydrocarbon mixes with water zone has low-resistivity values at 5.2 m depth. Spring water has leaked from outside the region through Kubaisah area. This explains the contaminated groundwater seepage within Hit area that was sited within the quaternary deposits and karst gypsum fractures of the study area.

Acknowledgement

The authors wish to thank the head and members of the Department of Applied Geology for the important geological information they provided to carry out this research. Likewise, they would like to thank the Dean of the College of Science (University of Anbar) for providing the SAS-4000 tool, electrodes, electrical cables, etc. that were necessary in conducting the field survey. They would also like to thank the Municipality of Hit for the outstanding scientific cooperation in accomplishing this research.

References

1. Hussien, B. M., Rabeea, M. A., and Farhan, M. M. **2016**. Characterization and behavior of Hydrogen Sulfide plumes released from active sulfide-tar springs, Hit-Iraq. *Atmospheric Pollution Research*, **2**: 1-10.
2. Waxman, M. H. and Thomas, E. C. **1974**. Electrical conductivities in shaly sands. I. The relation between hydrocarbon saturation and resistivity index. II. The temperature coefficient of electrical conductivity, *J. Petrol. Tech. Trans*. AIME, **257**: 213- 225.
3. Andres, K. G. and Canace, R. **1984**. Use of the electrical resistivity technique to delineate a hydrocarbon spill in the coastal plain deposits of New Jersey. Proc. of the NWWA/API Conf. on petroleum hydrocarbons and organic chemicals in ground water - prevention, detection and restoration, Houston, p.p. 188-197.
4. Sauck, W. A. **1998**. A conceptual model for the geoelectrical response of LNAPL plumes in granular sediments. Proceeding of the Symposium on the Application of Geophysics to Engineering and Environmental Problems, **11**: 805-817.
5. Sauck, W. A. **2000**. A model for the resistivity structure of LNAPL plumes and their environs in sandy sediments. *Journal of Applied Geophysics*, **44**: 151 -165.
6. Shevnin, V., Delgado-Rodríguez, O., Mousatov, A., Nakamura-Labastida, E. and Mejia-Aguilar, **2003**. Oil pollution detection using resistivity sounding. *Geofisica Internacional*, **42**(4): 613-622.
7. Shevnin, V., Delgado-Rodríguez, O., Fernández-Linares, L., Martínez, H. Z., Mousatov, A. and Ryjov, A. **2005**. Geoelectrical characterization of an oil-contaminated site in Tabasco, Mexico.

Geofísica Internacional, **44**(3): 251-263.

8. Atekwana, E. A., Atekwana, E. A., Rowe, R. S., Werkema, D. D. and Legall, F. D. **2004**. The relationship of total dissolved solids measurements to bulk electrical conductivity in an aquifer contaminated with hydrocarbon. *Journal of Applied Geophysics*, **56**: 281- 294.

9. Delgado-Rodríguez, O., Shevnin, V., Ochoa-Valdés, J. and Ryjov, A. **2006**. Geoelectrical characterization of a site with hydrocarbon contamination caused by pipeline leakage. *Geofísica Internacional*, **45**(1): 63-72.

10. Allen, J.P., Atekwana, E. A., Duris, J. W., Werkema, D. D. and Rossbach, S. **2007**. The Microbial Community Structure in Petroleum-Contaminated Sediments Corresponds to Geophysical Signatures. *Applied and Environmental Microbiology*, **73**(9): 2860-2870.

11. Uchegbulam O. and E. A. **2014**. Application of Electrical Resistivity Imaging in Investigating Groundwater Pollution in Sapele Area, Nigeria, *Journal of Water Resource and Protection*, **6**: 1369-1379.

12. Sadowski, R. M. **1988**. Clay-organic interactions. MSc. Thesis, Dept. of Geochemistry, Colo. School of Mines, Golden, CO, 209 p.

13. Mazáč, O., Benes, L., Landa, I. and Maskova, A. **1990**. Determination of the extent of oil contamination in groundwater by geoelectrical methods. Geotechnical and environmental geophysics, Vol. 2, Society of Exploration Geophysics, Tulsa, p. 107-112.

14. Barker, R., Rao, T.V., Thangarajan M. **2001**. Delineation of contaminant zone through electrical imaging technique. *Curr Sci*, **81**(3): 277–283.

15. Thabit, M. J. and Khalid, H., F. **2016**. Resistivity Imaging Survey to Delineate Subsurface Seepage of Hydrocarbon Contaminated Water at Karbala Governorate, Iraq. *Environmental Earth Sciences*, Springer. **75**(1): 75-87.

16. Abed, A. M. **2013**. Comparison between 2D electrical imaging survey and traditional electrode arrays in delineating subsurface cavities in Haditha-Hit area (Western Iraq). Ph.D. Thesis, Geology Department, Science College, Baghdad University, Baghdad, Iraq, pp: 120.

17. Thabit, J. M. and Abed, A. M. **2013**. Evaluation of different electrode arrays in delineation subsurface cavities by using 2D imaging technique, *J. of Univ. of Anbar for Pure Science*, **7**(3): 166-175.

18. Thabit, J. M., Abed, A. M. and Al-Menshed, F. H. **2015**. 3D resistivity imaging survey to delineating and mapping Um El-Githoaa cavity in Hit area. Western Iraq, *Tikrit journal of Pure Science*, **20**(2): 135-141.

19. Salman, A. M, Abed, A. M., and Thabit J. M. **2020**. Comparison between Dipole-dipole and Pole-dipole Arrays in Delineation of Subsurface Weak Zones Using 2D Electrical Imaging Technique in Al-Anbar University, Western Iraq, *Iraqi Journal of Science*, **61**(3): 567-576.

20. Jassim, S. Z. and Goff, J. **2006**. Geology of Iraq. Dolin, Prague and Moravian Museum, Brno.pp:341.

21. Al-Ghreri, M. F. T. **2007**. Bio stratigraphic succession of the formations in the upper Euphrates River in the area between Hit and Al-Qaim. Ph. D. Thesis, Geology Department, Science College, Baghdad University, Baghdad, Iraq: 13-16.

22. Al Dulaymi A., Hussein B., Gharbi A. H., and Mekhlif, H. N. **2013**. Balneological study based on the hydrogeochemical aspects of the sulfate springs water (Hit–Kubaiysa region), Iraq. *Arab J Geosci*, **6**: 801–81.

23. Hussien BM, Gharbi M. **2010a**. Hydrogeologic condition within AbuJir Fault Zone (Hit–Kubaiysa). *Iraqi Journal of Desert Studies*, **2**(2): Congress. ISSN 1994–7801.

24. Hussien BM, Gharbi M. **2010b**. Hydro geochemical evaluation of the ground water within Abu-Jir Fault Zone. I.B.G.M, ISSN 1811- 4539. *S.C OF G.S. M*., **6**(1).

25. Griffiths, D. H., Barker, R. D. **1993**. Two-dimensional resistivity imaging and modelling in areas of complex geology. *J Appl Geophys*, **29**(3–4): 211–226.

26. Al-Aslami, O. J. M. **2015**. Sedimentary facies and oil seeps characterization of Fatha Formation in west of Iraq. Msc. Unpublished MSc. thesis, science college, University of Baghdad: 51P.

27. Geotomo S. **2018**. RES2DINV version 4.9.15 Software Program of 2D Resistivity and IP Inversion Program. https://www.geotomosoft.com/downloads.php.

28. Loke, M. H. **2020**. Tutorial: 2-D and 3D electrical imaging surveys, *Geophys*, **10**(4): 339–349 E-mail:drmhloke@yahoo.com, geotomo@gmail.com, p 176.